Journal of Applied Physics

Inverse design of thermal metamaterials with holey engineering strategy

Cite as: J. Appl. Phys. **132**, 145102 (2022); https://doi.org/10.1063/5.0108743
Submitted: 10 July 2022 • Accepted: 14 September 2022 • Published Online: 11 October 2022

Zhaochen Wang, Zhan Zhu, Tianfeng Liu, et al.

AIP Publishing

Journal of Applied Physics ARTICLE scitation.org/journal/jap

Inverse design of thermal metamaterials with holey engineering strategy

Cite as: J. Appl. Phys. 132, 145102 (2022); doi: 10.1063/5.0108743
Submitted: 10 July 2022 · Accepted: 14 September 2022 ·
Published Online: 11 October 2022

Zhaochen Wang, Zhan Zhu, Tianfeng Liu, and Run Hu[a)]

AFFILIATIONS

School of Energy and Power Engineering, Huazhong University of Science and Technology, Wuhan 430074, China

[a)]**Author to whom correspondence should be addressed:** hurun@hust.edu.cn

ABSTRACT

Manipulating heat with thermal metamaterials has garnered increasing attention for enabling underlying physics and promising applications. However, the frequently adopted strategy to fabricate thermal metamaterials is using layered structures, whose design space is limited and, thus, other strategies demand further exploring. Here, we propose the holey engineering strategy as an alternative to design thermal metamaterials based on genetic algorithm optimization. The design procedures are introduced in detail, and two metadevices including the thermal cloak and thermal concentrator, are designed and verified to demonstrate the feasibility and convenience of this strategy. This work proposes a new design method for thermal metamaterials and paves an efficient way for macroscopic heat flow manipulation.

I. INTRODUCTION

Thermal metamaterials have been intensively explored as they offer superior advantages over the naturally occurring materials in terms of adjustable thermal conductivity, high design degree of freedom, and abundant underlying physics.[1–12] Based on thermal metamaterials, many novel thermal functionalities have been demonstrated theoretically and experimentally like cloaking,[13–17] concentrating,[18,19] illusion,[20–22] camouflage,[23,24] printing,[25] encoding,[26] etc. To design thermal metamaterials, the transformation thermotics theory is frequently applied, in which the designed thermal conductivity κ' is $\kappa' = \mathbf{J}\kappa_0\mathbf{J}^T/\det(\mathbf{J})$, where $\mathbf{J}$ is the Jacobian matrix of the coordinate transformation and κ_0 is the isotropic thermal conductivity of the background.[27–30] Due to the matrix operations, the designed thermal conductivity is an anisotropic tensor, which enables the anisotropic heat flow under the uniform heat flux input. The anisotropic tensor κ' is challenging to manufacture with the naturally occurring isotropic materials, and the compromised solution is mixing two different materials with proper ratios.[31–34] For instance, in our previous papers, we drilled holes and stripes in copper plate and filled with the mixture of boron nitride particles and epoxy, with varying filling ratio and stripe orientations.[20] As far as we can see that most experimental implementation of thermal metamaterials are fabricated by layered structures with effective media approximation. When fixed with two materials, the layered structures can only achieve two Wiener bounds (series and parallel bounds) and the remaining large space cannot be accessible.[5] So, can we design thermal metamaterials with other strategy?

In this study, we propose the holey engineering strategy as an alternative to design thermal metamaterials based on genetic algorithm (GA) optimization. We divide the design region into discrete unit cells and calculate the thermal conductivity tensor with transformation thermotics theory, and then design unit structures by drilling holes on copper plate, whose distribution is optimized by GA optimization. The design method for the unit structure is verified with the finite element method (FEM) simulation and two thermal functionalities, i.e., thermal cloaking and concentrating, are designed and demonstrated via FEM simulations, respectively. This study is expected to offer a new possibility for the design of thermal metamaterials and can be extended to other physical fields.

II. THEORETICAL DESIGN

We consider a two-dimensional system consisting of two concentric circles placed on a square background ($L \times L$), as shown in Fig. 1(a). The annual region is the design region of thermal metamaterials, and the central region is the target region for thermal functionalities. The radius of two concentric circles is R_1 and R_2, and the thermal conductivity of background and central region is κ_b. The thermal conductivity of the design region can be determined by the transformation thermotics theory according to the presupposed thermal functionalities. Here, we design a circular thermal

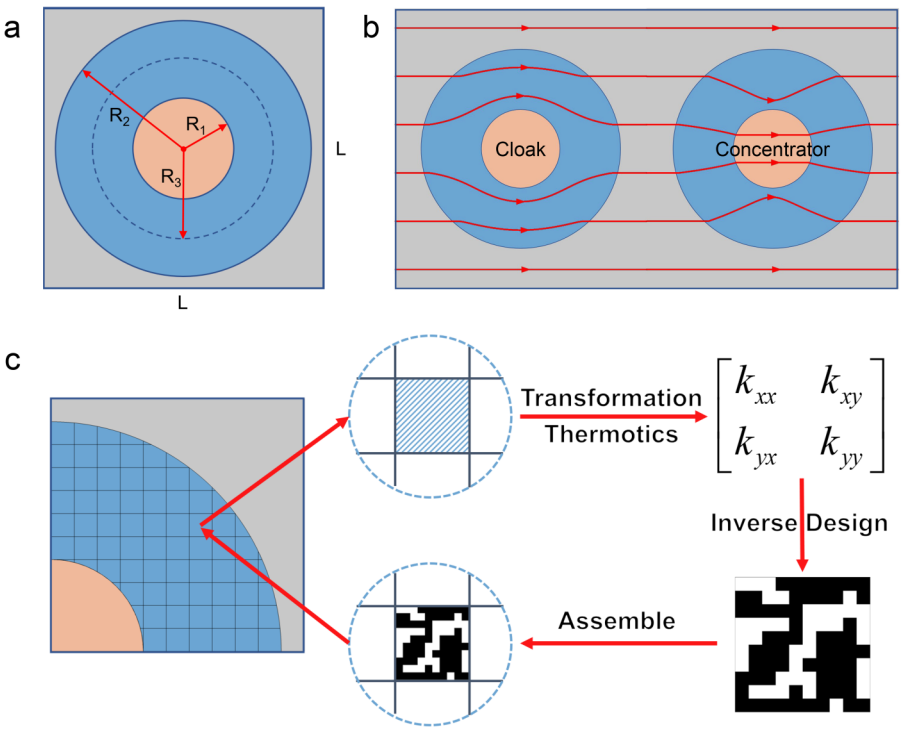

FIG. 1. Schematic diagram of (a) two-dimensional thermal functional system, (b) heat flow regulation with thermal cloak and thermal concentrator, (c) design method for thermal metamaterials with holey engineering strategy.

cloak and thermal concentrator for demonstration. A thermal cloak can render the central region invisible to the outside thermal flux, thereby resulting in a near-zero thermal gradient in the central region. In contrast, a thermal concentrator can attract heat flux to enter the central region, thereby resulting in a large thermal gradient in the central region. Both can achieve thermal functionalities without affecting the external field. In a cylindrical coordinate, the designed thermal conductivity tensor for thermal cloak is[27]

$$\kappa'_{\text{cloak}} = \begin{bmatrix} \kappa'_r & 0 \\ 0 & \kappa'_\theta \end{bmatrix} = \text{diag}\left(\frac{r'-R_1}{r'}, \frac{r'}{r'-R_1}\right)\kappa_b, \quad (1)$$

and for thermal concentrator, the designed thermal conductivity tensor is[27]

$$\kappa'_{\text{concentrator}} = \begin{bmatrix} \kappa'_r & 0 \\ 0 & \kappa'_\theta \end{bmatrix} = \text{diag}\left(\frac{r' + R_2\frac{R_3-R_1}{R_2-R_3}}{r'}, \frac{r'}{r' + R_2\frac{R_3-R_1}{R_2-R_3}}\right)\kappa_b, \quad (2)$$

where R_3 can be designed intermediate shape variable, by which we compress the inner part ($r' < R_3$) into the central region ($r' < R_1$) and stretch the outer part ($R_3 < r' < R_2$) into the original annular region ($R_1 < r' < R_2$), in order to maintain the consistency between the original space and the transformation space. From Eq. (1), we can see that when r' approaches R_1, the radial component κ'_r tends to be zero and the azimuth component κ'_θ tends to be infinite and singularity, thus heat cannot enter the central region, resulting in an isothermal and background-independent invisible performance, as shown in Fig. 1(b). On the contrary, the singularity problem is removed with inserting a proper R_3 function in Eq. (2), and the heat is directed into the central region of thermal concentrator resulting in a larger temperature gradient. From both Eqs. (1) and (2), we can see that the designed thermal conductivity tensors are strongly anisotropic and vary with coordinates, so the remaining challenge is how to design and fabricate such anisotropic metamaterials.

To tackle a such challenge, we propose the holey engineering strategy as a new approach, which is illustrated in Fig. 1(c). First, the design region of thermal metamaterials is divided into $n \times n$ unit cells, and then the thermal conductivity tensor of each unit cell can be calculated by Eqs. (1) and (2), according to the coordinates of the central point of the unit cell. In this way, we substitute the discrete thermal conductivity tensors in the discrete unit cells to represent the original circular design region to avoid the problem of continuous change of thermal conductivity with coordinates. Second, we employ GA optimization to obtain the specific holey structure of each unit cell whose effective thermal conductivity tensor equals to the calculated one, and the corresponding flow diagram is shown in Fig. 2. We choose two materials (with thermal conductivities κ_1 and κ_2) to construct metamaterial structures, and the two materials are represented by digits of 0 and 1, respectively. Each material distribution can be encoded as a 0–1 array, with the material distribution corresponding to the phenotype and the 0–1 array corresponding to the genotype in the GA. Then, M arrays of 0–1 is randomly generated as the initial population of GA, where

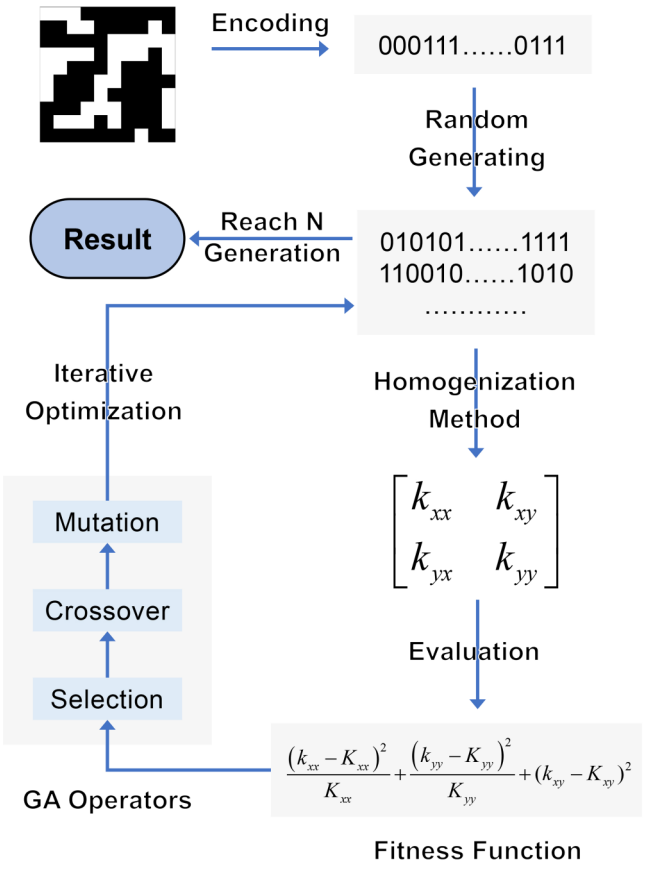

FIG. 2. Flow chart of inverse design of each unit cell based on GA optimization.

each 0–1 array is a chromosome. Thermal conductivity tensor of each chromosome can be quickly calculated by the homogenization method,[35] which can be expressed as $\begin{bmatrix} k_{xx} & k_{xy} \\ k_{yx} & k_{yy} \end{bmatrix}$. The fitness function F is used to evaluate the quality of each chromosome in the population, which is calculated by the following formula:

$$F = \frac{(k_{xx} - K_{xx})^2}{K_{xx}} + \frac{(k_{yy} - K_{yy})^2}{K_{yy}} + (k_{xy} - K_{xy})^2, \tag{3}$$

where $\begin{bmatrix} K_{xx} & K_{xy} \\ K_{yx} & K_{yy} \end{bmatrix}$ is the target thermal conductivity tensor by the transformation theory. After evaluating, three kinds of GA operators are employed to expand population, namely, selection, crossover, and mutation. Selection means some of the best chromosomes are selected to be passed on to the next generation, leaving the best chromosomes in each generation unaltered. Crossover refers to two chromosomes are cut off at the same position and the two strands cross to form two new chromosomes which will become two of the next generation. This operator is also known as gene recombination or hybridization, whose purpose is to find a better combination of gene segment for the next generation. Mutation refers to that some sudden changes may occur with a probability when a chromosome is passed on to the next generation, thereby resulting in the creation of new genes and the display of new traits. That is to say, chromosomes will change randomly with a low probability. This operator can improve the ability of random search and increase the diversity of the population. The above operators are used to continuously generate the next generation population in iterative optimization, where the probability of crossover and mutation are P_{cross} and P_{mutation}, respectively. After N iterations, the optimal result is the final chromosome, which will then be decoded into phenotype, and the metamaterial structure in each unit cell whose effective thermal conductivity equals to the target thermal conductivity tensor is obtained. Finally, after obtaining all the metamaterial in each unit cell, we assemble all the metamaterial structures into the designed metadevice according to the coordinates of their central positions.

III. RESULTS AND DISCUSSION

First, we evaluate the inverse design of each unit cell by comparing the temperature field of theoretical metamaterials and designed metamaterials. We set the target thermal conductivity tensor as $\kappa = \begin{bmatrix} 48.9 & 39.4 \\ 39.4 & 82.5 \end{bmatrix}$ W m^{-1} K^{-1} and simulate two cases in COMSOL Multiphysics. In the first case, a 50×50 mm^2 square plate is created and set the thermal anisotropy as the target thermal conductivity tensor $\kappa = \begin{bmatrix} 48.9 & 39.4 \\ 39.4 & 82.5 \end{bmatrix}$ W m^{-1} K^{-1} directly. The two boundaries perpendicular to the temperature gradient are set as 373 and 273 K, and the two boundaries parallel to the temperature gradient are set as adiabatic boundaries. In the second case, copper and air are selected as two materials in the GA inverse design. The GA optimization parameters are set as $M = 50$, $N = 100$, $P_{\text{cross}} = 0.9$, and $P_{\text{mutation}} = 0.1$. Then, after the GA inverse design, we obtain the structure for the target thermal conductivity tensor $\kappa = \begin{bmatrix} 48.9 & 39.4 \\ 39.4 & 82.5 \end{bmatrix}$ W m^{-1} K^{-1}. A 5×5 periodic holey structure is assembled whose hole size is 50×50 mm^2 as well. As is shown in Figs. 3(b) and 3(c), black represents copper with thermal conductivity of 400 W m^{-1} K^{-1} and white represents air with thermal conductivity of 0.026 W m^{-1} K^{-1}. Thermal convection is ignored and boundary conditions are the same as the first case.

The simulated temperature distributions when the uniform heat is input from x and y directions are shown as Figs. 3(d)–3(g), from which the overall temperature profiles of theoretical simulation and structural simulation are consistent. However, owing to the non-smooth copper structures, the temperature distribution of the structural simulation is not as uniform as that in the theoretical simulation. In order to further quantitatively analyze the temperature distribution, the corresponding temperature profiles along the diagonal line [gray dotted line in Figs. 3(d)–3(g)] are illustrated as Figs. 3(h) and 3(i). It can be observed that although the temperature profile in the theoretical simulation results is smooth and that in the structural simulation is zigzag, the trend of the two is basically the same. This difference is mainly due to the limited number

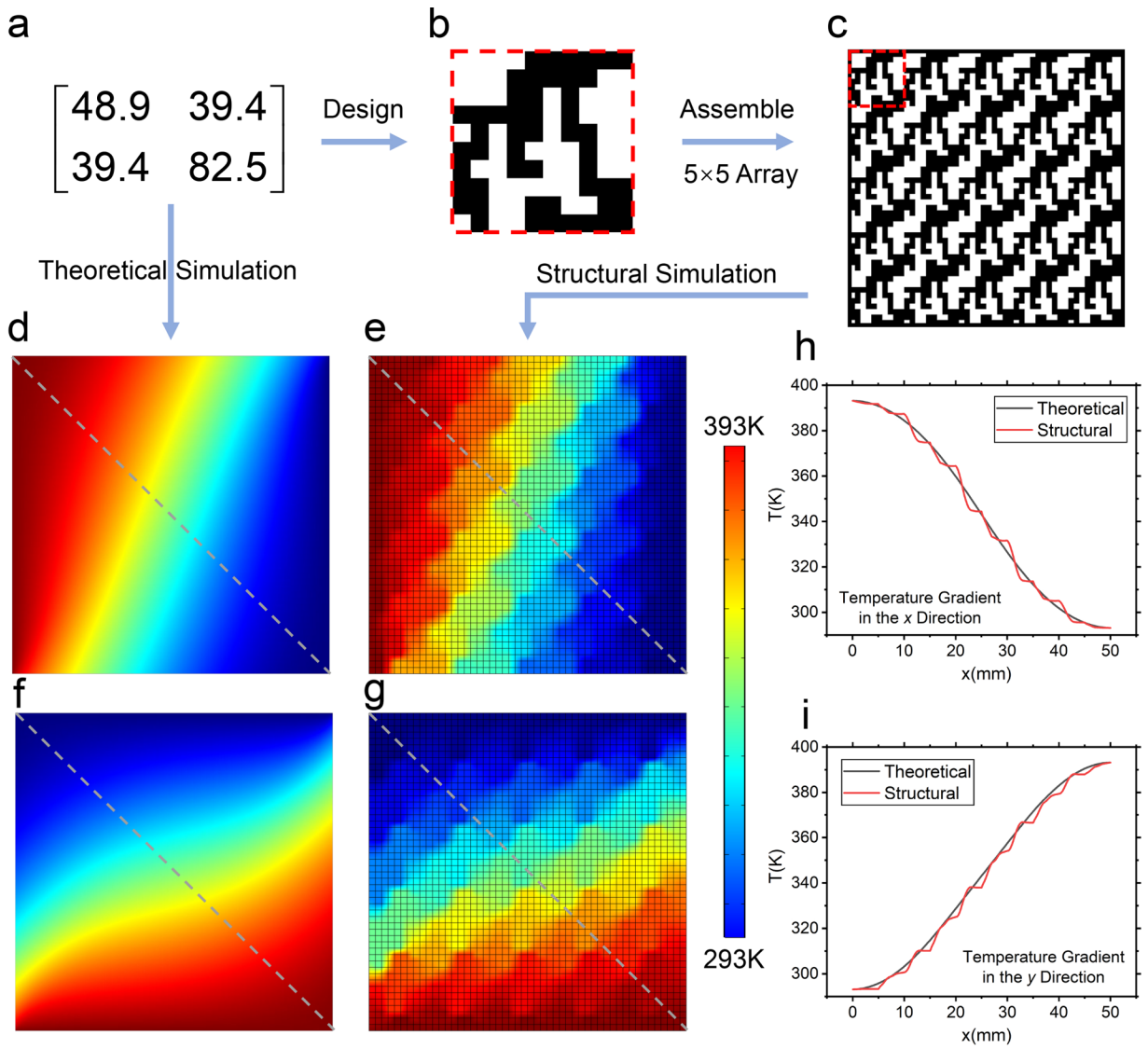

FIG. 3. Verifications for unit structure design method. (a) Target thermal conductivity tensor. (b) Designed structure of the unit cell. (c) Assembled structure of the 5 × 5 array. (d)–(g) Temperature distribution of theoretical simulation and structural simulation with temperature gradient in the x and y directions, respectively. (h) and (i) Temperature along the observational lines (gray dotted lines) in (d)–(g).

of unit cell, and the limited number of elements in each unit cell. The distribution of holes is optimized by GA, whose effective thermal conductivity tensor is approximated to the calculated tensor by transformation thermotics theory. But because of the abrupt change of thermal conductivity of copper and air, the corresponding temperature profile is not as smooth as the target field. To enhance the temperature smoothness, we can increase the number of unit cells and the number of elements in each unit cell as many as possible by balancing the accuracy and computation cost. In general, the above results show that the designed structure can largely achieve the heat flow regulation of theoretical anisotropic materials and verify the feasibility of the GA inverse design method for each unit cell.

In order to verify the effectiveness of the holey engineering strategy for thermal metamaterials, we then design thermal cloak and thermal concentrator for demonstration and evaluate the performance by FEM simulation. We take the following parameters: $\kappa_b = 20\ \mathrm{W\ m^{-1}\ K^{-1}}$, $L = 160$ mm, $R_1 = 20$ mm, $R_2 = 50$ mm, $R_3 = 35$ mm. Copper ($\kappa_{\mathrm{copper}} = 400\ \mathrm{W\ m^{-1}\ K^{-1}}$) and air ($\kappa_{\mathrm{air}} = 0.026\ \mathrm{W\ m^{-1}\ K^{-1}}$) are the two materials in GA optimization, and the optimization parameters are set as $M = 50$, $N = 100$, $P_{\mathrm{cross}} = 0.9$, and $P_{\mathrm{mutation}} = 0.1$. Following the design steps described

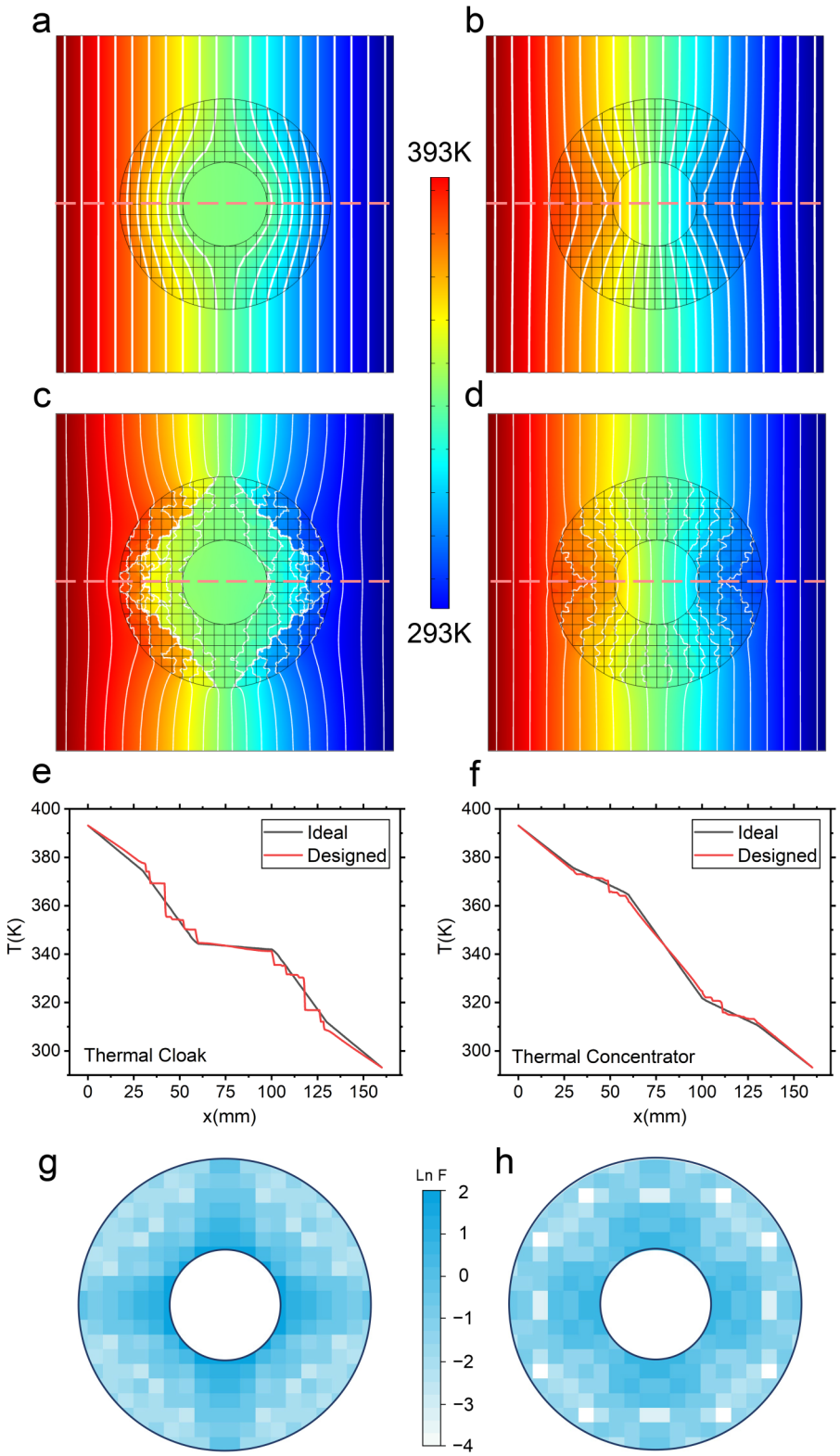

FIG. 4. Results of FEM simulation. (a) and (b) Temperature distribution of thermal cloak and thermal concentrator in an ideal situation. (c) and (d) Temperature distribution of the designed thermal cloak and thermal concentrator. (e) and (f) Temperature along the observational lines (red dotted lines) in (a)–(d). (g) and (h) Error distribution of designed thermal cloak and thermal concentrator.

above, the circular region is divided into 20×20 unit cells and the size of each unit cell is $10 \times 10\ \mathrm{mm}^2$. The thermal conductivity tensor of each unit cell is calculated and the structure of each unit cell is designed and assembled together. FEM simulation is performed by COMSOL Multiphysics. The left and right sides of the plate are set as 373 and 273 K, respectively, and the upper and lower sides of the plate are adiabatic boundaries.

We first show the theoretical simulation temperature fields of thermal cloak and concentrator in Figs. 4(a) and 4(b), respectively, in which the thermal conductivity tensor is calculated by the transformation theory. The structural simulation of designed metamaterials with a specific holey structure is shown in Figs. 4(c) and 4(d). It is seen that the temperature distribution of the designed thermal cloak is similar to that of theoretical situation. As for thermal cloak, the isotherms bypass the central region, and the temperature gradient of central region is only $63.528\ \mathrm{K\,m^{-1}}$ which is 80% smaller than that in the background of $312.5\ \mathrm{K\,m^{-1}}$. As for thermal concentrator, the isotherms in the design region converge to the center region, and the isotherms in the central region are significantly denser than that in the background, with a temperature gradient of $453.92\ \mathrm{K\,m^{-1}}$, 45% higher than that in the background. Comparing theoretical and structural simulations, whether it is a thermal cloak or a thermal concentrator, the temperature profile in the background and central region on the red dotted line in Figs. 4(a)–4(d) are basically the same, as shown in Figs. 4(e) and 4(f). The temperature curve within the design region is stepped due to the huge difference in thermal conductivity of copper and air, but still exhibits the same trend as the theoretical situation. Observing the external isotherms, the isotherms around the thermal cloak are not completely parallel but are slightly perturbed by the metadevices, which is different from the theoretical situation. As for thermal concentrators, the perturbation is relatively small and negligible, and the external isotherms are nearly parallel. It is worth mentioning that, owing to the fact that this holey structure can be represented by a 0–1 matrix, which is in good agreement with GA, the calculation speed of this design method is very fast. It takes only about 2h with CPU Intel i 5 10400 to design the entire thermal functional device. Overall, the designed metamaterials with holey structures show good thermal functionalities as transformation theory and offer a general "discretion-and-assembly" strategy to design thermal metamaterials.

Further, we would like to discuss more on the error of the thermal conductivity tensor. Considering the distribution of the components K_{xx}, K_{yy}, and K_{xy} (K_{yx}) of thermal conductivity tensor $\kappa = \begin{bmatrix} K_{xx} & K_{xy} \\ K_{yx} & K_{yy} \end{bmatrix}$, the closer the unit cell is to the central region, the larger the thermal conductivity tensor value and the anisotropy, as summarized by Eqs. (1) and (2). This significant anisotropy leads to difficulties in the design of unit cells close to the central region, as more complex and special structures are required. In Figs. 4(g) and 4(h), the fitness function of each unit cell in the design region is illustrated, which can be regarded as the design error of each unit cell. The fitness function of the unit cells next to the central region is much higher than that of the unit cells far away, which means that these unit cells have a larger error in the GA inverse design, while the other unit cells are designed with higher accuracy. These large or small errors combine to make the overall thermal conductivity of thermal functional device deviate from the thermal conductivity of background, resulting in non-parallel isotherms in the background. Compared with the thermal cloak, the thermal concentrator has less anisotropy, thus the design error is smaller, making the background isotherms more parallel. However, from an overall perspective, the error of most design unit cells is small, so the influence on the overall heat flow regulation is acceptable, and good thermal functionalities can still be achieved.

IV. CONCLUSION

In this study, we proposed the holey engineering strategy based on the GA optimization, as an alternative method to design thermal metamaterials beyond the conventional layered strategy. The merits of the holey engineering strategy include, without a prior knowledge of the background temperature field, large design freedom, high efficiency, traversing the full-parameter space, etc. The thermal cloak and thermal concentrator are designed in this way and their performance has been verified by FEM simulations, which is close to the ideal design by the transformation theory. This present method can be used to design other metamaterials with different functionalities even with extremely complex shapes, as long as the discrete unit cells are small enough. This work provides a new avenue for thermal metamaterial design and arbitrary heat flow manipulation and can be easily extended to other physical fields for both metamaterials and metadevices.

ACKNOWLEDGMENTS

The authors acknowledge financial support from the National Natural Science Foundation of China (NNSFC) (Grant Nos. 52076087, 5216110332, and 5221150005), Wuhan City Science and Technology Program (Grant No. 2020010601012197), and the Wuhan City Knowledge Innovation Shuguang Program.

AUTHOR DECLARATIONS

Conflict of Interest

The authors have no conflicts to disclose.

Author Contributions

Zhaochen Wang: Conceptualization (equal); Investigation (equal); Methodology (equal); Writing – original draft (equal). **Zhan Zhu:** Data curation (equal); Investigation (equal); Methodology (equal). **Tianfeng Liu:** Validation (equal). **Run Hu:** Conceptualization (equal); Funding acquisition (equal); Supervision (equal); Writing – review & editing (equal).

DATA AVAILABILITY

The data that support the findings of this study are available from the corresponding author upon reasonable request.

REFERENCES

[1]S. Guenneau, C. Amra, and D. Veynante, "Transformation thermodynamics: Cloaking and concentrating heat flux," Opt. Express **20**, 8207–8218 (2012).

[2]Y. Li, K. J. Zhu, Y. G. Peng, W. Li, T. Yang, H. X. Xu, H. Chen, X. F. Zhu, S. Fan, and C. W. Qiu, "Thermal meta-device in analogue of zero-index photonics," Nat. Mater. **18**, 48–54 (2019).
[3]J. Li, Y. Li, P. C. Cao, T. Yang, X. F. Zhu, W. Wang, and C. W. Qiu, "A continuously tunable solid-like convective thermal metadevice on the reciprocal line," Adv. Mater. **32**, e2003823 (2020).
[4]J. Li, Y. Li, W. Wang, L. Li, and C. W. Qiu, "Effective medium theory for thermal scattering off rotating structures," Opt. Express **28**, 25894–25907 (2020).
[5]W. Sha, R. Hu, M. Xiao, S. Chu, Z. Zhu, C. W. Qiu, and L. Gao, "Topology-optimized thermal metamaterials traversing full-parameter anisotropic space," npj Comput. Mater. **8**, 179 (2022).
[6]L. Xu and J. Huang, "Controlling thermal waves with transformation complex thermotics," Int. J. Heat Mass Transf. **159**, 120133 (2020).
[7]C. Z. Fan, Y. Gao, and J. P. Huang, "Shaped graded materials with an apparent negative thermal conductivity," Appl. Phys. Lett. **92**, 251907 (2008).
[8]M. Moccia, G. Castaldi, S. Savo, Y. Sato, and V. Galdi, "Independent manipulation of heat and electrical current via bifunctional metamaterials," Phys. Rev. X **4**, 021025 (2014).
[9]X. Shen, Y. Li, C. Jiang, and J. Huang, "Temperature trapping: Energy-free maintenance of constant temperatures as ambient temperature gradients change," Phys. Rev. Lett. **117**, 055501 (2016).
[10]X. Shen, C. Jiang, Y. Li, and J. Huang, "Thermal metamaterial for convergent transfer of conductive heat with high efficiency," Appl. Phys. Lett. **109**, 201906 (2016).
[11]R. Hu, S. Zhou, W. Shu, B. Xie, Y. Ma, and X. Luo, "Directional heat transport through thermal reflection meta-device," AIP Adv. **6**, 125111 (2016).
[12]Y. Su, Y. Li, T. Yang, T. Han, Y. Sun, J. Xiong, L. Wu, and C. W. Qiu, "Path-dependent thermal metadevice beyond Janus functionalities," Adv. Mater. **33**, e2003084 (2021).
[13]T. Han, X. Bai, D. Gao, J. T. Thong, B. Li, and C. W. Qiu, "Experimental demonstration of a bilayer thermal cloak," Phys. Rev. Lett. **112**, 054302 (2014).
[14]Y. Li, X. Shen, Z. Wu, J. Huang, Y. Chen, Y. Ni, and J. Huang, "Temperature-dependent transformation thermotics: From switchable thermal cloaks to macroscopic thermal diodes," Phys. Rev. Lett. **115**, 195503 (2015).
[15]T. Han, P. Yang, Y. Li, D. Lei, B. Li, K. Hippalgaonkar, and C. W. Qiu, "Full-parameter omnidirectional thermal metadevices of anisotropic geometry," Adv. Mater. **30**, e1804019 (2018).
[16]Z. Zhu, X. Ren, W. Sha, M. Xiao, R. Hu, and X. Luo, "Inverse design of rotating metadevice for adaptive thermal cloaking," Int. J. Heat Mass Transf. **176**, 121417 (2021).
[17]T. Chen, C.-N. Weng, and J.-S. Chen, "Cloak for curvilinearly anisotropic media in conduction," Appl. Phys. Lett. **93**, 114103 (2008).
[18]Y. Li, X. Shen, J. Huang, and Y. Ni, "Temperature-dependent transformation thermotics for unsteady states: Switchable concentrator for transient heat flow," Phys. Lett. A **380**, 1641–1647 (2016).
[19]X. Shen, Y. Li, C. Jiang, Y. Ni, and J. Huang, "Thermal cloak-concentrator," Appl. Phys. Lett. **109**, 031907 (2016).
[20]R. Hu, S. Zhou, Y. Li, D. Y. Lei, X. Luo, and C. W. Qiu, "Illusion thermotics," Adv. Mater. **30**, e1707237 (2018).
[21]W. Sha, Y. Zhao, L. Gao, M. Xiao, and R. Hu, "Illusion thermotics with topology optimization," J. Appl. Phys. **128**, 045106 (2020).
[22]S. Zhou, R. Hu, and X. Luo, "Thermal illusion with twinborn-like heat signatures," Int. J. Heat Mass Transf. **127**, 607–613 (2018).
[23]Y. Li, X. Bai, T. Yang, H. Luo, and C. W. Qiu, "Structured thermal surface for radiative camouflage," Nat. Commun. **9**, 273 (2018).
[24]R. Hu, W. Xi, Y. Liu, K. Tang, J. Song, X. Luo, J. Wu, and C. W. Qiu, "Thermal camouflaging metamaterials," Mater. Today. **45**, 120–141 (2021).
[25]R. Hu, S. Huang, M. Wang, X. Luo, J. Shiomi, and C. W. Qiu, "Encrypted thermal printing with regionalization transformation," Adv. Mater. **31**, e1807849 (2019).
[26]R. Hu, S. Huang, M. Wang, L. Zhou, X. Peng, and X. Luo, "Binary thermal encoding by energy shielding and harvesting units," Phys. Rev. Appl. **10**, 054032 (2018).
[27]X. Y. Shen and J. P. Huang, "Transformation thermotics: Thermal metamaterials and their applications," Acta Phys. Sin. **65**, 178103 (2016).
[28]Y. Li, W. Li, T. Han, X. Zheng, J. Li, B. Li, S. Fan, and C. W. Qiu, "Transforming heat transfer with thermal metamaterials and devices," Nat. Rev. Mater. **6**, 488–507 (2021).
[29]X. Xu and B. Li, "Transformation thermotics and the manipulation of thermal energy," Opto-Elec. Eng. **44**, 64–68 (2017).
[30]S. Yang, J. Wang, G. Dai, F. Yang, and J. Huang, "Controlling macroscopic heat transfer with thermal metamaterials: Theory, experiment and application," Phys. Rep. **908**, 1–65 (2021).
[31]J. Li, Y. Li, T. Li, W. Wang, L. Li, and C.-W. Qiu, "Doublet thermal metadevice," Phys. Rev. Appl. **11**, 044021 (2019).
[32]G. Xu, K. Dong, Y. Li, H. Li, K. Liu, L. Li, J. Wu, and C. W. Qiu, "Tunable analog thermal material," Nat. Commun. **11**, 6028 (2020).
[33]S. Kang, J. Cha, K. Seo, S. Kim, Y. Cha, H. Lee, J. Park, and W. Choi, "Temperature-responsive thermal metamaterials enabled by modular design of thermally tunable unit cells," Int. J. Heat Mass Transf. **130**, 469–482 (2019).
[34]W. Sha, M. Xiao, J. Zhang, X. Ren, Z. Zhu, Y. Zhang, G. Xu, H. Li, X. Liu, X. Chen, L. Gao, C. W. Qiu, and R. Hu, "Robustly printable freeform thermal metamaterials," Nat. Commun. **12**, 7228 (2021).
[35]E. Andreassen and C. S. Andreasen, "How to determine composite material properties using numerical homogenization," Comput. Mater. Sci. **83**, 488–495 (2014).